Desalination and Water Treatment
www.deswater.com
doi: 10.5004/dwt.2020.25170

188 (2020) 159–168
June

Sulfate-containing wastewater treatment, electricity generation and community structure in an anaerobic fluidized bed–microbial fuel cell

Jibai Wang, Youxian Gao, Shuxin Liu, Qin Cai, Changmiao Lai, Ping Yang*

College of Architecture and Environment, Sichuan University, Chengdu 610065, China, Tel. +86 18408258462; emails: yangpinga301@163.com (P. Yang), wjbscu@163.com (J. Wang), 619813598@qq.com (Y. Gao), 360708835@qq.com (S. Liu), 1823395572@qq.com (Q. Cai), 425656390@qq.com (C. Lai)

Received 22 May 2019; Accepted 13 November 2019

ABSTRACT

A large amount of wastewater containing high concentration sulfate is discharged from the industrial production process. Wastewater with a high concentration of sulfate and low chemical oxygen demand (COD)/SO_4^{2-} ratio is difficult to biodegrade. An anaerobic fluidized bed–microbial fuel cell (AFB–MFC) system was constructed to illustrate the effects of high sulfate concentration and low COD/SO_4^{2-} ratio on anodic system performance. Results showed that, with increased SO_4^{2-} concentration from 900 to 7,200 mg/L and COD from 6,000 to 2,400 mg/L, COD, NH_4^+–N and SO_4^{2-} removal efficiency decreased from 95.9% to 52.5%, 43.3% to 28.5%, 81.2% to 18.6%, respectively. When SO_4^{2-} was 3,600 mg/L, the maximum output voltage of 704.6 mV and a power density of 24.8 mW/m^2 were achieved, respectively. Meanwhile, sludge characteristics analyses revealed a high concentration of SO_4^{2-} addition had little effect on microbial sedimentation performance of the AFB–MFC system. Genomic sequencing analysis of anode bioparticles revealed that increasing sulfate altered *Levilinea* from 2.12% to 16.3%, which co-worked with *Methanolinea* while suppressing *Methanosaeta* thereby adapting to substrate adjustment. The studies would be conducive to the development of AFB–MFC applications in the treatment of high sulfate concentration wastewater.

Keywords: Anaerobic fluidized bed; Community structure; Electricity generation; Microbial fuel cell system; Sulfate wastewater

1. Introduction

Many industries, including chemical, pharmaceutical, papermaking, and mining processes [1,2], discharge large amounts of wastewater containing a high concentration of organics and sulfate [3]. Anaerobic biotechnology has been widely used to treat a high concentration of organic wastewater because it is cost-effective and environmentally-friendly [4]. However, a high concentration of sulfate will lead to the proliferation of sulfate-reducing bacteria (SRB), which is not conducive to biological treatment. On the one hand, sulfate-reducing produces sulfide, while both total dissolved sulfide and free H_2S promote an adverse effect on microbes, reactor operation and pipeline [5]. On the other hand, SRB competes with methane-producing bacteria (MPB) for electrons from organics degradation, thus affecting the performance of the system. It has been widely accepted that the influent chemical oxygen demand (COD)/SO_4^{2-} ratio would affect the dominant species (MPB and SRB) in the anaerobic reactor, which is important for organics removal and sulfate reduction [6,7]. Theoretically, the sulfate can be completely reduced when COD/SO_4^{2-} ratio over 0.67, COD becomes a limiting factor, resulting in a decrease in sulfate reduction efficiency at COD/SO_4^{2-} of 0.5 at an anaerobic reactor [8]. Hu et al. [6] revealed the conversion of influent COD to methane dropped from 80.5 to 54.4% by decreasing COD/SO_4^{2-} ratio from 20 to 0.5 in the upflow anaerobic sludge blanket reactors. Therefore, finding a reactor that can operate at a

* Corresponding author.

low COD/SO_4^{2-} ratio and withstand the effects of sulfides is significant.

Microbial fuel cell (MFC) is a novel bioelectrochemical system for the recovery of energy and nutrients from various organic waste streams [9]. In MFC, organic compounds are oxidized by microorganisms while the produced electrons are transferred to the external circuit to output electric energy. When the MFC is applied in treating sulfur-containing wastewater, the electrochemical properties of MFC can reduce the hazard of sulfide to the entire system. In general, sulfide concentration above 150 mg/L in wastewater is toxic to MPB [3]. However, Rabaey et al. [10] reported H_2S generated in situ in an MFC would be expected to be rapidly oxidized to sulfur. H_2S is an electron donor, which gives off its electrons to the oxidant with the most positive redox potential (anode electrode), and elemental sulfur is formed in the anode chamber as a by-product [11]. Meanwhile, hydrogen sulfide as an electron donor can make the anode potential more negative, which is beneficial to electricity generation [12]. Therefore, due to its unique energy environment effect and sulfate adaptability, MFC has been used in sulfate-containing wastewater where studies have been carried out on denitrifying sulfide removal, operating conditions, bioelectricity generation, etc. [12–14]. However, there is still a gap of knowledge about responses of morphology and microbial communities to influence COD/SO_4^{2-} ratios since a low COD/SO_4^{2-} ratio will still yield poor MFC performance [15].

To improve and to assess the performance of MFC on treating organic wastewater containing high sulfate, a continuous-flow MFC system was constructed. We transformed the anode chamber of the traditional dual-chamber MFC into an anaerobic fluidized bed (AFB) reactor, and the cathode chamber adopted an aerobic biocathode. The anaerobic biological particles, which had been formed in the AFB in the previous experiment [16], were beneficial to the sufficient contact between microorganisms and wastewater [17]. Meanwhile, the application of such systems in treating sulfate wastewater has not been reported. Hence, the main objective of this work was to confirm the effectiveness of anaerobic fluidized bed–microbial fuel cell (AFB–MFC) in the treatment of sulfate wastewater. The pollutant removal and power generation of the anode under different stages were investigated. Additionally, the responses of extracellular polymeric substances (EPS) production and microbial communities to sulfate which governs the performance of the AFB–MFC system were analyzed in this study.

2. Materials and methods

2.1. MFC configuration, media and operational condition

In this experiment, a two-chamber MFC system made of plexiglass was constructed (Fig. 1), with an AFB (10.66 L effective volume) as the anode chamber and aerobic biocathode (9.96 L aeration zone + 3.81 L sedimentation zone) as the cathode chamber. The anode and cathode were separated by a proton exchange membrane (PEM, Nafion 117, Dupond, USA). Both the anode and cathode electrodes were made of porous carbon paper (HCP030, an effective area of 200 cm^2). The anode chamber (dug up a portion of the wall) was attached to a porous (7 × 15 hole) plexiglass plate (180 × 450 mm). The cathode chamber (dug up a portion of the wall as well) was connected to the other side of the porous plexiglass plate. The PEM was sandwiched between the sidewall of the cathode chamber and the plexiglass plate. In the anode AFB reactor, porous polymer-carriers were used as the nuclei of the anaerobic biological particles [18], which accounted for approximately 1/6 (v/v) of the anode chamber. The hydraulic retention time (HRT) of AFB was controlled at 24 h while the temperature was controlled at 35°C ± 1°C. Feedwater was mixed with the effluent from the upper part of the AFB bioreactor (4.6 L/h) through the reflux pump, and the water was evenly fed from the bottom of the reactor. The external resistance was fixed at 1 kΩ, and the output voltage was recorded by a computer connected to a UT70B multimeter.

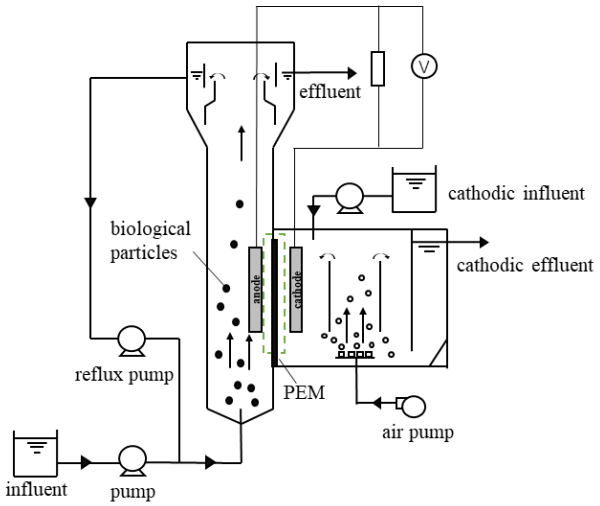

Fig. 1. AFB–MFC system set-up.

2.2. Experimental wastewater and reactor operating parameters

Synthetic wastewater was used in this study. The main components of water distribution contained $C_6H_{12}O_6$, $(NH_4)_2SO_4$, KH_2PO_4, Na_2SO_4 and trace element (1 mL/L of each nutrient solution, Table S1). The operating parameters of MFC treating wastewater containing sulfate are shown in Table 1. To measure the high SO_4^{2-} concentration and different COD/SO_4^{2-} ratios on the performance of the AFB–MFC system, the experiment was divided into two phases (Table S2). Stage I–V were the phase 1 by raising the influent sulfate concentration (from 900; 1,800; 3,600; 5,400 to 7,200 mg/L) while VI–VIII were the phase 2 by decreasing the influent COD concentration (from 6,000; 4,800; 3,600 to 2,400 mg/L).

2.3. Analysis and calculation

Concentrations of COD, NH_4^+–N, NO_3^- and NO_2^- were measured according to the standard methods [19]. The removal efficiency is $(E_a/E_c) = (C_0–C_1)/C_0 \times 100\%$, where C_0 (mg/L) is the concentration of the influent and C_1 (mg/L) is the concentration of the anode effluent. SO_4^{2-} concentration was measured by ion chromatography using a Dionex

Table 1
Operating parameters of the AFB–MFC system

Phase	1	2
Anaerobic COD load, g/L d	6.0	6.0–2.4
Anaerobic NH_4^+–N load, g/L d	0.210	0.210–0.084
Anaerobic SO_4^{2-} load, g/L d	0.9–7.2	7.2
Anaerobic HRT, h	24	24
Anaerobic reflux rate, L/h	7.2	7.2
Aerobic COD load, g/L d	2.5	2.5
Aerobic reflux rate, L/h	1.24	1.24
Cathode dissolved oxygen, mg/L	6.5–7.0	6.5–7.0

ICS-1100 (Thermo Fisher Scientific Inc., MA, USA). S^{2-} concentration was measured by an iodometric titration method. The extraction of total EPS was heated at 80°C for 20 min, centrifuged at 4,000 r/min for 15 min, and then passed through a 0.45 um aqueous phase membrane. The polysaccharides (PS) were detected by the phenol-sulfuric acid method while proteins (PN) were determined by the Lowry method [20]. Voltage was measured by a digital multimeter at definite time intervals and the volumetric power density was calculated as $P = U^2/RA$, where U is the recorded voltage (V), R is the external resistance (Ω) and A is the surface area of the anode electrode (m^2).

2.4. Microbial community analysis

Microbial communities in the granule sludge at stage II and V were investigated using 16S rRNA amplicon sequencing. 2 ml of the per samples were taken and centrifuged at 4,500 rpm for 15 min, and the precipitated DNA was taken. E.Z.N.ATM Mag-Bind Soil DNA kit (Omega Bio-tek, Inc., Norcross, GA, USA) was used for DNA extraction. The total DNA was extracted from the granular sludge according to the instructions, and DNA integrity was detected by an agarose gel. Accurate quantification of genomic DNA used the Qubit2.0 DNA Assay Kit. For archaea, three-wheeled PCR amplification was used. The first round was amplified using M-340F and GU1ST-1000R as the primers. The second round was amplified using the products of the first round, and the primers used for PCR have been fused to the V3-V4 universal primers of the Miseq sequencing platform. For the third round of amplification, Illumina Bridge PCR compatible primers were introduced. For bacterial, the first round used the universal bacterial primers 341F and 805R to amplify the V1-V3 region of the 16S rRNA gene of the extracted DNA, and the Illumina bridge PCR compatible primers were introduced in the second round. After PCR amplification, the amplicons were extracted from agarose gel using the AxyPrep DNA Gel Extraction Kit (Axygen Biosciences, Union City, CA, USA). DNA was accurately quantified by using the Qubit2.0 DNA detection kit and mixed in an equal amount of 1:1, then sequenced on the machine. Software used for sequencing was Prinseq, FLASH, Mothur, Uclust, Cytoscape, Oiime, Muscle, MEGAN, RDP, Fasttree. The database used for the sequencing was the RDP classifier database, the Silva database, and the Unite database.

3. Results and discussion

3.1. Effects of sulfate on the treatment performance in the anode

3.1.1. COD removal

The COD concentrations and removal efficiency of the anode under different phases are shown in Fig. 2a. In phase 1, influent COD at a concentration of 6,000 mg/L was used. By increasing the influent SO_4^{2-} concentration, the effluent COD concentration increased continuously (from 245.4 to 1,058.1 mg/L), corresponding to a removal efficiency from 95.9% to 82.4%. When influent SO_4^{2-} concentration reached 7,200 mg/L, the concentration of S^{2-} in the effluent increased continuously (state in 3.1.3), thus stopped increasing the concentration of SO_4^{2-} and gradually reduced the concentration of the influent COD. The influent COD varied from 4,800; 3,600 to 2,400 mg/L in phase 2, corresponding to a COD/SO_4^{2-} ratio of 0.67, 0.50 and 0.33. In this phase, the COD removal efficiency decreased from 71.7% to 52.5%, which was worse than that in phase 1.

The reason for the variety in COD removal could be explained in two ways, microbial competition and sulfide toxicity. First, the sulfate reduction was weak in initial stages and the SRB could degrade the accumulation of propionic acid [21], and the system achieved a high COD removal efficiency of over 90%. In the later stages, increasing sulfate promoted the enrichment of SRB. Since SRB owns higher kinetic and thermodynamic advantages [22], and the sulfate reduction process generally takes precedence over the methanogenesis process [23], SRB could usually compete over MPB. Moreover, lower COD/SO_4^{2-} ratio (<0.67) in phase 2 would affect normal anaerobic digestion and reduce system stability [24], which was manifested by a decrease in COD removal. Second, sulfide produced after sulfate reduction in the anaerobic environment. Initially, less sulfide was formed and could be quickly oxidized at the anode. Meanwhile, a suitable concentration of sulfides was beneficial to the system. (a) Sulfide maintains the lower oxidation-reduction potential of the anode. (b) Sulfide can be used as a source for MPB growth. (c) Sulfide can precipitate Cu^{2+}, Ni^{2+}, Zn^{2+} and other heavy metals that are toxic to anaerobic microorganisms [25]. However, in the later stages, with the accumulation of large amounts of sulfide, the excess sulfide could form cross-links among polypeptide chains, denature proteins, and interfere with key enzyme metabolism in the cells [26], thus reducing the stability of the system. It is worth noting that the COD removal efficiency of the whole system could still be kept above 50% even when the COD/SO_4^{2-} ratio drops to 0.33.

3.1.2. Ammonium removal

In phase 1, the influent NH_4^+–N concentration was displayed at 210 mg/L. With SO_4^{2-} addition, the removal efficiency of NH_4^+–N decreased continuously, from an average of 43.3% to 28.5%, with the corresponding amount of NH_4^+–N removal decreased from 90.9 to 59.9 mg/L (Fig. 2b). The decrease of NH_4^+–N removal efficiency was caused by two possible ways. (1) SO_4^{2-} became an active electron acceptor. As the dominant species, SRB suppressed the activity of nitrifying bacteria and denitrification. (2) Increasing sulfide

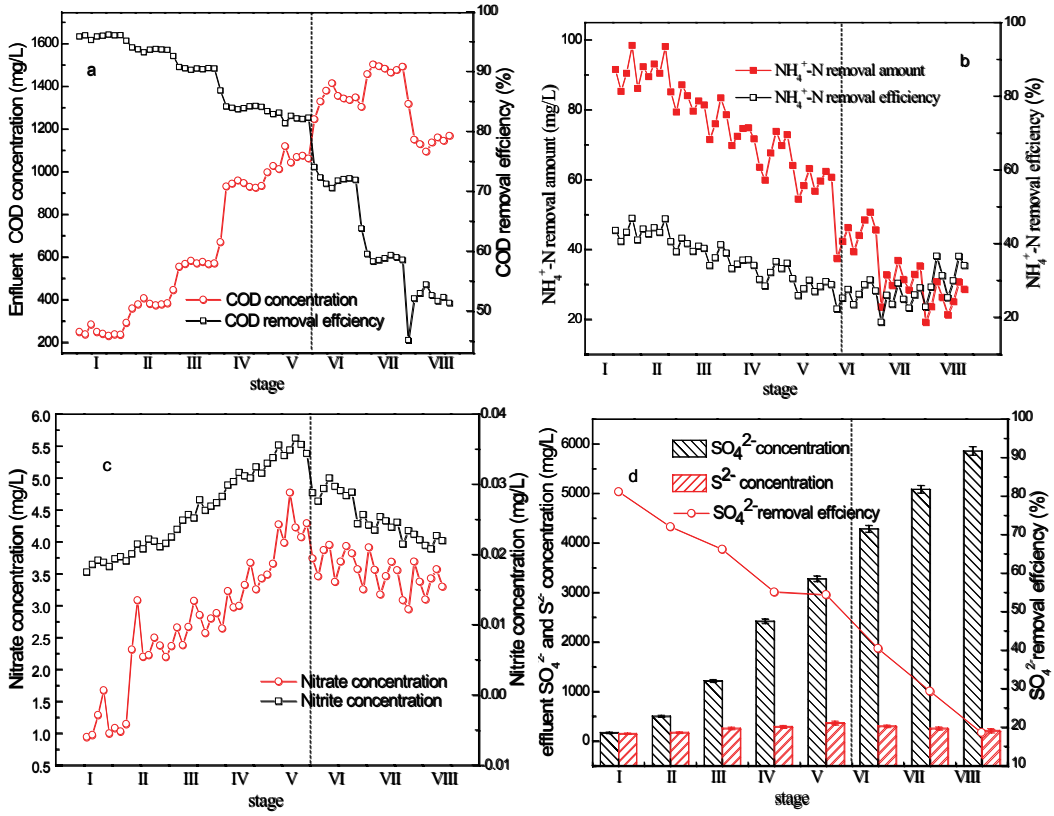

Fig. 2. Variations of anaerobic effluent COD (a), NH_4^+–N (b), NO_3^-–N and NO_2^-–N (c), SO_4^{2-} and S^{2-} (d) under different stages.

was toxic to nitrifying bacteria, which reduced NH_4^+–N removal efficiency [27]. In phase 2, as influent COD reduced to 2,400 mg/L, the influent NH_4^+–N was decreased in the same proportion, from 210 to 84 mg/L. With the decrease of N/SO_4^{2-}, the removal efficiency increased slightly (from 28.5% to 31.7%), however, the amount of NH_4^+–N removal continued to decrease (from 59.9 to 26.7 mg/L).

Besides, a small amount of nitrite and nitrate were detected in samples of different stages in the AFB reactor (Fig. 2c). Possible explanations of nitrite and nitrate generation could be concluded in three ways. (a) Autotrophic nitrification occurred at the anode since oxygen influx through the influent. (b) Partial ammonium could be directly oxidized on the anode electrode [16]. (c) Sulfate-type anaerobic ammonium oxidation reaction could occur as follows [28].

$$3SO_4^{2-} + 4NH_4^+ \rightarrow 3S^{2-} + 4NO_2^- + 4H_2O + 8H^+ \quad (1)$$

$$NO_2^- + O_2 \rightarrow NO_3^- \quad (2)$$

However, the main factor in nitrate and nitrite accumulation cannot be confirmed. Chen et al. [29] noted the heterotrophic nitrification was markedly inhibited when sulfide exceeded 200 mg/L, resulting in nitrite accumulation and subsequent destruction of the denitrification system. In addition, with SO_4^{2-} increased, the SRB competed over denitrifying bacteria for electronic donors, resulting in the gradual accumulation of nitrate and nitrite.

3.1.3. SO_4^{2-} removal and S^{2-} production

The study demonstrates that MFC has the special capability of combining sulfate reduction and sulfide oxidation [10]. SO_4^{2-} and S^{2-} in the effluent with different influent concentrations of SO_4^{2-} were detected, and the results are shown in Fig. 2d. In phase 1, sulfate addition was exceeded the amount of sulfate that the system could remove, and the removal efficiency of SO_4^{2-} in anode decreased (from 81.2 to 54.5%). Meanwhile, the amount of removed SO_4^{2-} increased from 730.6 to 3921.0 mg/L, with the corresponding effluent S^{2-} concentration increasing from 133.6 to 344.4 mg/L. Chatterjee et al. [3] reported that sulfide concentration did not inhibit anodic biochemical reactions in MFCs, due to instantaneous abiotic oxidation to sulfur. However, in our studies, there was still a cumulative accumulation of sulfides. It was probably due to the relatively small proportion of electrode in the entire reactor and the continuous deposition of S^0 on the electrode resulted in the reduction of effective electrode area, thus the sulfide in the anodic chamber could not be completely oxidized.

As MPB was inhibited by sulfides and SRB could grow in acetate and ethanol with high concentrations of sulfides (IC_{50}~1,300 mg/L H_2S) [26,30], and the amount of sulfate reduction continued to increase. In phase 2, as organics decreased, removal efficiency of SO_4^{2-} decreased from 54.5% to 18.6%, while S^{2-} production decreased from 344.41 to 209.6 mg/L. The continuous reduction of COD/SO_4^{2-} ratio led to a reduction in the supply of electrons to SO_4^{2-} reduction

thus resulted in the rapid decline in SO_4^{2-} removal and S^{2-} produced.

Furthermore, it can be easily seen from Table 2 the ratio of $S^{2-}_{production}/SO^{2-}_{4removal}$ was changed from 0.207 to 0.093 and then elevated to 0.156, comparing to a theoretical value of 0.33 (S^{2-}/SO_4^{2-} = 0.33). The declining ratios confirmed the occurrence of sulfide oxidation. Sulfide was oxidized to sulfur while sulfur was further oxidized to thiosulfate, sulfite and sulfate [13].

As a conclusion, the possible mechanisms of desulfurization in the anode were illustrated in Fig. 3 according to the above experimental phenomena in 3.1. (a) Microorganisms absorbed sulfate as a nutrient to synthesize important sulfur-containing organic compounds, such as cysteine [31]. (b) Sulfate was reduced to sulfide by SRB. (c) H_2S gas was generated and discharged outside of the reactor and absorbed by the lye. (d) Sulfide oxidation by sulfur-oxidizing bacteria (SOB). (e) Sulfide was simultaneously desulfurized and denitrified with NO_2^- and NO_3^- to form N_2 and S^0 by sulfur denitrifying bacteria [32]. (f) S^0 was formed due to electrochemical oxidation of sulfide.

Table 2
Variations of anaerobic $S^{2-}_{production}/SO^{2-}_{4removal}$ in different stages

Stage	$S^{2-}_{production}/SO^{2-}_{4removal}$
I	0.207
II	0.133
III	0.108
IV	0.097
V	0.093
VI	0.103
VII	0.121
VIII	0.156

3.2. Electricity generation of the AFB–MFC reactor for treating organic wastewater containing sulfate

Initially, the output voltage and power density increased from 662.5 to 704.6 mV and 21.9 to 24.8 mW/m² with SO_4^{2-} addition (Fig. 4). The elevation can be directly correlated to the increasing sulfate ion concentration, which led to an increase in electrical conductivity. Wei et al. [33] noted that suitable sulfate addition increased the amount of electricity generated at startup. Furthermore, sulfide oxidation is one of the key players in electricity generation in sediment systems [10]. The accumulation of sulfide led to a decrease in the anode potential while the residual sulfate and sulfide formed as a soluble redox mediator, which assisted electrons transfer and increased the electricity generation

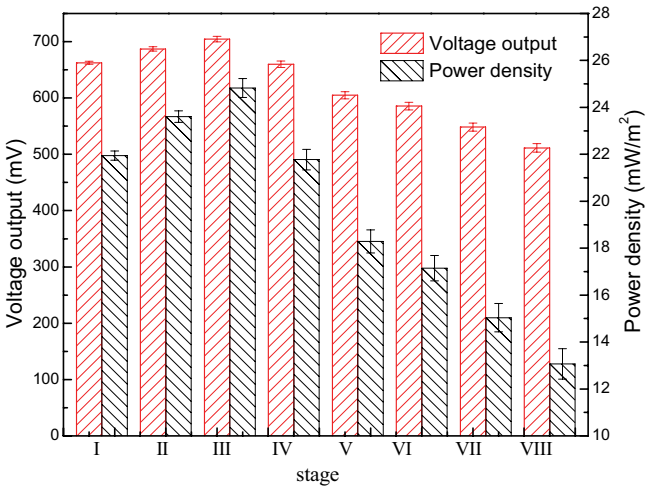

Fig. 4. Variations of voltage output and power density output under different stages.

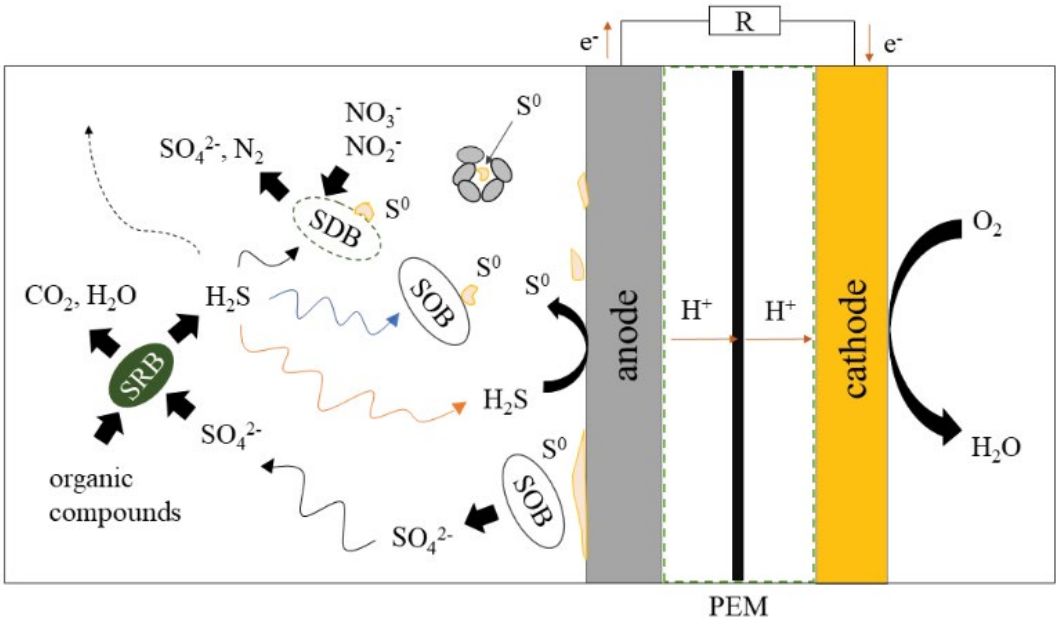

Fig. 3. Proposed mechanism of desulfurization in the anode of AFB–MFC.

[34]. At an SO_4^{2-} concentration of 7,200 mg/L, more SO_4^{2-} competed with electrodes for electrons, thus hindering the electricity generation [35]. Moreover, the accumulated of sulfide in AFB had a toxic effect on electrogenic bacteria [36], which decreased the voltage output (from 704.6 to 604.8 mV). As influent organics decreased in phase 2, the voltage dropped sharply to 511.3 mV at influent COD of 2,400 mg/L. It might be caused by the reduction of electron donors provided by organic matter, and the electrons transferred to the anode were reduced. In addition, the solid sulfur gradually formed on PEM (Nafion), preventing the attachment of protons to the membrane itself. This mechanism, known as Nafion scaling, together with the growth of the sludge on the membrane, leads to membrane saturation, which ultimately prevents cations and protons from participating in the cathodic reaction. Moreover, Nafion has negatively-charged chemical groups that attract positive ions in the organic substrate [37]. Because only H^+ can pass through the PEM, other positive ions accumulate on the membrane, which prevented further passage of H^+. The accumulation of protons at the anode resulted in a decrease in cathode function, which lowered the pH (from the initial pH of 7.54 to the final 7.02) of the anode reactor as in turn. In summary, the output voltage and power density of this experimental stage showed a trend of initial increase and followed by a decrease.

3.3. Sludge characteristics

3.3.1. Mixed liquid suspended solids and mixed liquor volatile suspended solids

As shown in Fig. 5a, in phase 1, both the mixed liquid suspended solids (MLSS) and mixed liquor volatile suspended solids (MLVSS) of anaerobic sludge in anode increased, from 46.4 to 54.1 g/L and 40.6 to 42.3 g/L, respectively. Related to adaptability, the upward trend of MLSS and MLVSS were gradually increased. At this phase, the number of SRB increased, and the sulfate-reducing activity was significantly enhanced. When SO_4^{2-} further increased to 7,200 mg/L, solid sulfur appeared in the effluent. The color of the sludge became deeper while the smell of H_2S became obvious. Thereafter, based on the growth rate and the accumulation of sulfide, the growth of microorganisms slowed down in phase 2, and the MLSS and MLVSS were decreased slightly.

Specifically, the ratio of MLVSS/MLSS declined throughout the experimental period, from the initial 87.7% to 74.2%. This might be related to the increase of S^0 in the structure of the microorganisms. However, the biomass of the anode still kept at a high level, which was an important reason for the high efficiency obtained in the AFB–MFC system.

3.3.2. Extracellular polymeric substances

EPS plays a key role in particle formation and stabilization. Studies have shown that high salinity concentrations have a significant effect on the structure of microbial EPS [38]. To further investigate the influences of sulfate on community structure, the EPS were extracted and the main components of PS, as well as PN, were analyzed. The results under different phases are summarized in Fig. 5b. At per stage, the concentration of PS and PN increased first and followed by a decrease (data not shown). The initial elevation might be caused by the acclimatization of microorganisms while the microorganisms had a process of adapting to sulfate.

In phase 1, the PS and PN increased from 18.6 to 31.6 mg/g MLVSS, 19.8 to 31.9 mg/g MLVSS, respectively. These results indicated microbes secreted more EPS to alleviate adverse environments under the environmental stimulus. By contrary, in phase 2, the PS and PN decreased from 28.29 to 21.2 mg/g MLVSS, 27.06 to 22.29 mg/g MLVSS. With the reduction of influent carbon and nitrogen, the capacity of the carbon and nitrogen source that the microorganism could absorb and utilize was reduced. Hence, the secretions, excretions, hydrolysates, and metabolites of the cells themselves were decreased, resulting in the decline in PN and PS content.

Furthermore, the ratio of PN/PS decreased slightly with sulfate increased. Generally, higher PN/PS values contribute to sludge flocculation by increasing the hydrophobicity of the particles [39]. The slight decline indicated sulfate addition made little detrimental in sludge sedimentation performance. In addition, the solid sulfur produced by sulfate reduction might be used as a nucleus by microorganisms

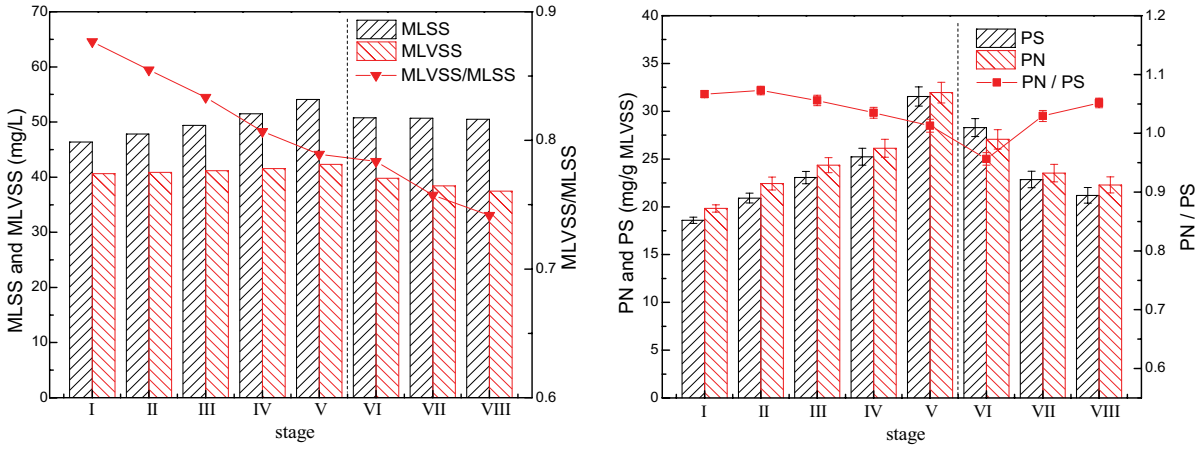

Fig. 5. MLSS and MLVSS in the anode (a), PS and PN in anodic EPS (b).

to promote the formation of the particles. Therefore, during the whole experiment, the sludge in the anode chamber had good sedimentation performance, even when influent sulfate concentration reached 7,200 mg/L, there was no phenomenon of sludge floating up.

3.4. Microbial community analysis of anode

To further investigate the effects of SO_4^{2-} on microbial community diversity, genomic sequencing analysis was performed on the anaerobic biological particles with SO_4^{2-} at 1,800 mg/L (stage II) and 7,200 mg/L (stage V). Results showed that, for bacteria (Table 3a and Fig. 6a), *Actinomyces* was most frequently detected (33.7%/27.5%), followed by *Anoxybacter* (25.8%/18.0%), *Mesotoga* (10.3%/12.2%), *Desulfomonile* (5.25%/6.07%), *Desulfomicrobium* (4.16%/6.94%), *Desulfovibrio* (3.4%/5.29%) and *Levilinea* (2.12%/16.3%).

Actinomyces naeslundii sp., *Mesotoga infera* sp. and *Anoxybacter fermentans* sp. were hydrolyzed acid-producing bacteria. *Actinomyces naeslundii* sp. requires CO_2 as a growth factor, which has also been reported in the anode chamber of MFC treating palm oil mill effluent wastewater [40]. Meanwhile, *Mesotoga infera* sp. is a medium-temperature anaerobic bacterium, which can utilize complex organic compounds, amino acids and glucose to reduce S^0 to S^{2-} [41,42]. *Levilinea saccharolytica* sp. is a mesophilic multicellular microorganism. It can provide abundant electron donors and carbon source materials for SRB through the metabolites of anaerobic fermentation.

Apart from the fermentation bacterium, SRB also played an important role in the anode community. *Desulfomicrobium baculatum* sp. belongs to the group of incomplete organic oxidizers, which oxidizes propionic acid and lactic acid to acetic acid by utilizing sulfate, sulfite and thiosulfate as the electron acceptors [1]. Most species of *Desulfomonile* can autotrophically grow in the presence of H_2 and CO_2 with sulfate or thiosulfate as the terminal electron acceptor. It can also utilize pyruvic acid and formate, reducing sulfate simultaneously [43]. *Desulfovibrio giganteus* sp. played a great role in organic substrates degrading and sulfate reduction, which also present in this system treating ammonium/organics rich wastewater [16]. As acclimation time increased, the proportion of SRB in the community increased, more SRB were domesticated and stored in the anode microbial community. It is worth noting that *Levilinea saccharolytica* sp. was gradually accounted for an important proportion in microbial communities from 2.12% to 16.3% due to its beneficial effect for providing SRB with abundant carbon source and electron donors.

It has been widely accepted that anodic sulfide oxidation in MFC was mediated by both abiotic and biotic processes. However, the SOB (such as *Paracoccus* sp., *Pseudomonas* sp. and *Rhodobacter* sp.) were not shown in the microbial community. Since anodic sulfide oxidation occurred as the formation of sulfur production, it could be concluded the sulfide oxidation to sulfur in the AFB–MFC system was mainly mediated by the abiotic process. Moreover, the most common electrogenic bacteria *Geobacter* sp. was also not found in this test [44]. The differences can be explained by the different samples taken, which were not from the electrode biofilm but the anaerobic biological particles in the anode chamber.

By contrast, archaea communities exhibited much less diversity than bacterial communities. In the archaea (Table 3b and Fig. 6b), almost all archaea were anaerobic methanogens, as *Methanolinea* (65.3%/76.3%) dominated, followed by *Methanosaeta* (26.9%/11.2%), *Methanobacterium* (4.13%/7.49%), and *Methanospirillum* (2.07%/1.46%). *Methanolinea tarda* sp. is a strictly anaerobic, Gram-negative bacterium and capable of utilizing H_2 and formate as electron donors for methane production. Scheller et al. [45] reported that the terminal electron acceptors for anaerobic oxidation of methane include sulfate and nitrate, which promotes the growth together with SRB. As a result, the relative abundance of *Methanolinea* and

Table 3a
Summary of bacterial phylotypes retrieved from anode chamber at different SO_4^{2-} concentration

Operation conditions	Abundance %	Closest cultured species (NCBI Accession) % homology	Class
Stage II	33.7	*Actinomyces naeslundii* strain 97	*Actinomycetaceae*
	25.8	*Anoxybacter fermentans* strain 95	*Halanaerobiales*
	10.3	*Mesotoga infera* strain VNS100 99	*Kosmotogaceae*
	5.25	*Desulfomonile tiedjei* strain DSM 96	*Desulfomicrobiaceae*
	4.16	*Desulfomicrobium baculatum* sp. 100	*Desulfomicrobiaceae*
	3.4	*Desulfovibrio giganteus* strain DSM 100	*Syntrophaceae*
	2.12	*Levilinea saccharolytica* strain KIBI-1 97	*Anaerolineaceae*
Stage V	27.5	*Actinomyces naeslundii* strain 97	*Actinomycetaceae*
	18.0	*Anoxybacter fermentans* strain 95	*Halanaerobiales*
	16.3	*Levilinea saccharolytica* strain KIBI-1 97	*Anaerolineaceae*
	12.2	*Mesotoga infera* strain 99	*Kosmotogaceae*
	6.94	*Desulfomicrobium baculatum* sp. 100	*Desulfomicrobiaceae*
	6.07	*Desulfomonile tiedjei* strain DSM 96	*Desulfomicrobiaceae*
	5.29	*Desulfovibrio giganteus* strain DSM 100	*Desulfovibrionaceae*

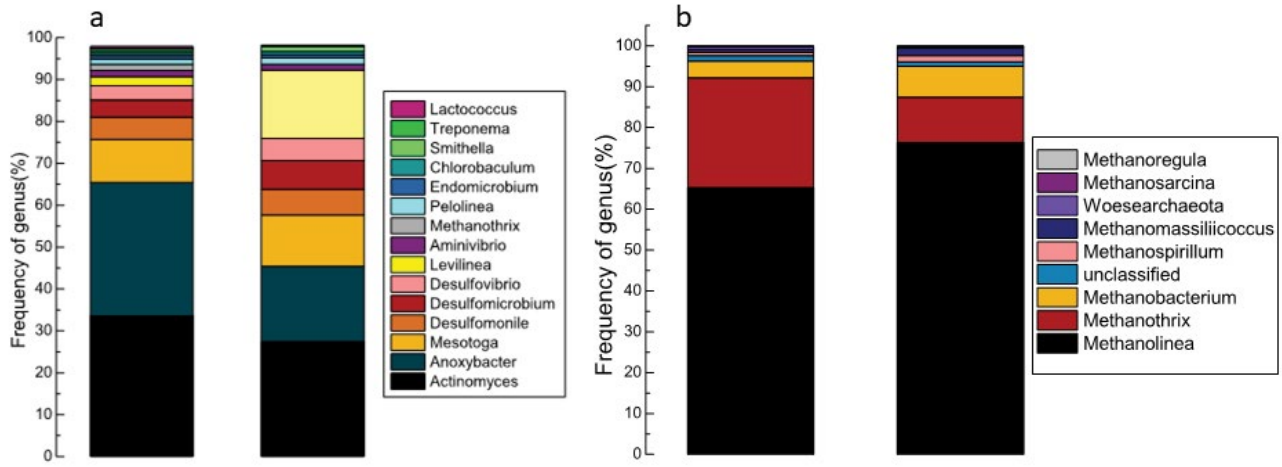

Fig. 6. Categories and abundance of genus of bacteria (a) and archaea (b) in anode chamber as SO_4^{2-} concentrations of stage II and V.

Table 3b
Summary of bacteria phylotypes retrieved from anode chamber at different SO_4^{2-} concentration

Operation conditions	Abundance %	Closest cultured species (NCBI Accession) % homology	Class
Stage II	65.3	*Methanolinea tarda* strain NOBI-1T 97	*Methanoregulaceae*
	26.9	*Methanosaeta concilii* 100	*Methanothrix*
	4.13	*Methanobacterium formicicum* strain BRM9 99	*Methanobacteria*
	2.07	*Methanospirillum hungatei* strain JF-1 98	*Methanomicrobia*
Stage v	76.3	*Methanolinea tarda* strain NOBI-1T 97	*Methanoregulaceae*
	11.2	*Methanosaeta concilii* 100	*Methanothrix*
	7.49	*Methanobacterium formicicum* strain BRM9 99	*Methanobacteria*
	1.46	*Methanospirillum hungatei* strain JF-1 98	*Methanomicrobia*

Methanobacterium increased. However, *Methanosaeta concilii* sp. could use acetate as the sole source of carbon and energy along with methane production [46], which might in part explain the inhibited observed with increasing sulfate load.

4. Conclusion

The AFB–MFC system was subjected to increasing sulfate and decreasing COD load where the pollutant treatment performance and power generation capacity was explored. The COD and NH_4^+–N removal efficiency dropped from 95.9% to 52.5% and 43.3 to 28.5%, while voltage output increased from 662.5 to 704.6 mV and followed by a drop to 511.3 mV, suggesting COD/SO_4^{2-} ratio below 0.67 has a greater impact on the performance of AFB–MFC. Sulfide oxidation to sulfur in the AFB–MFC system was mainly mediated by the abiotic process and sulfate addition made little detrimental in sludge sedimentation. Increasing SO_4^{2-} altered *Levilinea* from 2.12% to 16.3%, which provoked the *Methanolinea* but suppressed *Methanosaeta*.

Acknowledgment

This research was supported by the Science and Technology Support Program of Sichuan Province [2015SZ0009].

References

[1] T.W. Hao, P.Y. Xiang, H.R. Mackey, K. Chi, H. Lu, H.K. Chui, M.C. van Loosdrecht, G.H. Chen, A review of biological sulfate conversions in wastewater treatment, Water Res., 65 (2014) 1–21.
[2] M. Madani, M. Aliabadi, B. Nasernejad, R.K. Abdulrahman, M.Y. Kilic, K. Kestioglu, Treatment of olive mill wastewater using physico-chemical and Fenton processes, Desal. Wat. Treat., 53 (2013) 2031–2040.
[3] P. Chatterjee, M.M. Ghangrekar, S. Rao, S. Kumar, Biotic conversion of sulphate to sulphide and abiotic conversion of sulphide to sulphur in a microbial fuel cell using cobalt oxide octahedrons as cathode catalyst, Bioprocess. Biosyst. Eng., 40 (2017) 759–768.
[4] L.C. Reyes-Alvarado, A. Hatzikioseyian, E.R. Rene, E. Houbron, E. Rustrian, G. Esposito, P.N.L. Lens, Hydrodynamics and mathematical modelling in a low HRT inverse fluidized-bed reactor for biological sulphate reduction, Bioprocess. Biosyst. Eng., 41 (2018) 1869–1882.
[5] A. Sarti, M. Zaiat, Anaerobic treatment of sulfate-rich wastewater in an anaerobic sequential batch reactor (AnSBR) using butanol as the carbon source, J. Environ. Manage., 92 (2011) 1537–1541.
[6] Y. Hu, Z. Jing, Y. Sudo, Q. Niu, J. Du, J. Wu, Y.Y. Li, Effect of influent COD/SO_4^{2-} ratios on UASB treatment of a synthetic sulfate-containing wastewater, Chemosphere, 130 (2015) 24–33.
[7] B. Zhang, J. Zhang, Q. Yang, C. Feng, Y. Zhu, Z. Ye, J. Ni, Investigation and optimization of the novel UASB–MFC integrated system for sulfate removal and bioelectricity

generation using the response surface methodology (RSM), Bioresour. Technol., 124 (2012) 1–7.
[8] X. Lu, G. Zhen, J. Ni, T. Hojo, K. Kubota, Y.Y. Li. Effect of influent COD/SO_4^{2-} ratios on biodegradation behaviors of starch wastewater in an upflow anaerobic sludge blanket (UASB) reactor, Bioresour. Technol., 214 (2016) 175–183.
[9] P. Yang, W. Liao, H. Li, Aerobic granular sludge formation and COD removal in a continuous-flow microbial fuel cell, Desal. Wat. Treat., 129 (2018) 189–193.
[10] K. Rabaey, K.V.D. Sompel, L. Maignien, N. Boon. Microbial fuel cells for sulfide removal, Environ. Sci. Technol., 40 (2006) 5218–5224.
[11] A. Angelov, S. Bratkova, A. Loukanov, Microbial fuel cell based on electroactive sulfate-reducing biofilm, Energy Convers. Manage., 67 (2013) 283–286.
[12] D.J. Lee, X. Liu, H.L. Weng, Sulfate and organic carbon removal by microbial fuel cell with sulfate-reducing bacteria and sulfide-oxidising bacteria anodic biofilm, Bioresour. Technol., 156 (2014) 14–19.
[13] K. Wang, S. Zhang, Z. Chen, R. Bao, Interactive effect of electrode potential on pollutants conversion in denitrifying sulfide removal microbial fuel cells, Chem. Eng. J., 339 (2018) 442–449.
[14] L. Zhong, S. Zhang, Y. Wei, R. Bao, Power recovery coupled with sulfide and nitrate removal in separate chambers using a microbial fuel cell, Biochem. Eng. J., 124 (2017) 6–12.
[15] M.M. Ghangrekar, S.S.R. Murthy, M. Behera, N. Duteanu, Effect of sulfate concentration in the wastewater on microbial fuel cell performance., Environ. Eng. Manage. J., 9 (2010) 1227–1234.
[16] S. Liu, L. Li, H. Li, H. Wang, P. Yang, Study on ammonium and organics removal combined with electricity generation in a continuous flow microbial fuel cell, Bioresour. Technol., 243 (2017) 1087–1096.
[17] J. Guo, Y. Kang, Characterization of sulfate-reducing bacteria anaerobic granular sludge and granulometric analysis with grey relation, Korean J. Chem. Eng., 35 (2018) 1829–1835.
[18] J. Huang, P. Yang, Y. Guo, K. Zhang, Electricity generation during wastewater treatment: an approach using an AFB–MFC for alcohol distillery wastewater, Desalination, 276 (2011) 373–378.
[19] APHA, Standard Methods for the Examination of Water and Wastewater, 20th ed., Persulfate Method, APHA, AWWA & WEF, Washington, 1998.
[20] Z. Wang, M. Gao, Z. She, S. Wang, C. Jin, Y. Zhao, S. Yang, L. Guo, Effects of salinity on performance, extracellular polymeric substances and microbial community of an aerobic granular sequencing batch reactor, Sep. Purif. Technol., 144 (2015) 223–231.
[21] W. Qiao, K. Takayanagi, Q. Li, M. Shofie, F. Gao, R. Dong, Y.Y. Li, Thermodynamically enhancing propionic acid degradation by using sulfate as an external electron acceptor in a thermophilic anaerobic membrane reactor, Water Res., 106 (2016) 320–329.
[22] X. Lu, J. Ni, G. Zhen, K. Kubota, Y.Y. Li, Response of morphology and microbial community structure of granules to influent COD/SO_4^{2-} ratios in an upflow anaerobic sludge blanket (UASB) reactor treating starch wastewater, Bioresour. Technol., 256 (2018) 456–465.
[23] R.J.W. Meulepas, C.G. Jagersma, Y. Zhang, M. Petrillo, H. Cai, C.J. Buisman, A.J. Stams, P.N. Lens, Trace methane oxidation and the methane dependency of sulfate reduction in anaerobic granular sludge, FEMS Microbiol. Ecol., 72 (2010) 261–271.
[24] M.H.R.Z. Damianovic, E. Foresti, Anaerobic degradation of synthetic wastewaters at different levels of sulfate and COD/sulfate ratios in horizontal-flow anaerobic reactors (HAIB), Environ. Eng. Sci., 24 (2007) 383–393.
[25] V.F.D. Albuquerque, A.L.D. Barros, A.C. Lopes, A.B. dos Santos, R.F. do Nascimento, Removal of the metal ions Zn^{2+}, Ni^{2+}, and Cu^{2+} by biogenic sulfide in UASB reactor and speciation studies, Desal. Wat. Treat., 51 (2013) 2093–2101.
[26] J.L. Chen, R. Ortiz, T.W. Steele, D.C. Stuckey, Toxicants inhibiting anaerobic digestion: a review, Biotechnol. Adv., 32 (2014) 1523–1534.
[27] C. Huiliñir, R. Medina, S. Montalvo, A. Castillo, L. Guerrero, Biological nitrification in the presence of sulfide and organic matter: effect of zeolite on the process in a batch system, J. Chem. Technol. Biotechnol., 93 (2018) 2390–2398.
[28] F. Fdz-Polanco, M. Fdz-Polanco, N. Fernandez, M.A. Urueña, P.A. Garcia, S. Villaverde, New process for simultaneous removal of nitrogen and sulphur under anaerobic conditions, Water Res., 35 (2001) 1111–1114.
[29] C. Chen, A. Wang, N. Ren, H. Kan, D.J. Lee, Biological breakdown of denitrifying sulfide removal process in high-rate expanded granular bed reactor, Appl. Microbiol. Biotechnol., 81 (2008) 765–770.
[30] H. Greben, J. Maree, E. Eloff, K. Murray, Improved sulphate removal rates at increased sulphide concentration in the sulphidogenic bioreactor, Water SA, 31 (2005) 351–358.
[31] G. Na, D.E. Salt, The role of sulfur assimilation and sulfur-containing compounds in trace element homeostasis in plants, Environ. Exp. Bot., 72 (2011) 18–25.
[32] H. Pauwels, V. Ayraud-Vergnaud, L. Aquilina, J. Molénat, The fate of nitrogen and sulfur in hard-rock aquifers as shown by sulfate-isotope tracing, Appl. Geochem., 25 (2010) 105–115.
[33] L. Wei, H. Han, J. Shen, Effects of temperature and ferrous sulfate concentrations on the performance of microbial fuel cell, Int. J. Hydrogen Energy, 38 (2013) 11110–11116.
[34] I. Ieropoulos, J. Greenman, C. Melhuish, J. Hart, Energy accumulation and improved performance in microbial fuel cells, J. Power Sources, 145 (2005) 253–256.
[35] G. Liu, S. Yu, H. Luo, R. Zhang, S. Fu, X. Luo, Effects of salinity anions on the anode performance in bioelectrochemical systems, Desalination, 351 (2014) 77–81.
[36] F. Zhao, N. Rahunen, J.R. Varcoe, A.J. Roberts, C. Avignone-Rossa, A.E. Thumser, R.C.T. Slade, Factors affecting the performance of microbial fuel cells for sulfur pollutants removal, Biosens. Bioelectron., 24 (2009) 1931–1936.
[37] N. Jannelli, R. Anna Nastro, V. Cigolotti, M. Minutillo, G. Falcucci, Low pH, high salinity: too much for microbial fuel cells?, Appl. Energy, 192 (2017) 543–550.
[38] S.F. Corsino, M. Capodici, M. Torregrossa, G. Viviani, Physical properties and extracellular polymeric substances pattern of aerobic granular sludge treating hypersaline wastewater, Bioresour. Technol., 229 (2017) 152–159.
[39] R. Campo, S.F. Corsino, M. Torregrossa, G.D. Bella, The role of extracellular polymeric substances on aerobic granulation with stepwise increase of salinity, Sep. Purif. Technol., 195 (2017) 12–20.
[40] Y.L. Kang, S. Pichiah, S. Ibrahim, Facile reconstruction of microbial fuel cell (MFC) anode with enhanced exoelectrogens selection for intensified electricity generation, Int. J. Hydrogen Energy, 42 (2017) 1661–1671.
[41] X. Zeng, Z. Zhang, X. Li, X. Zhang, J. Cao, M. Jebbar, K. Alain, Z. Shao, *Anoxybacter fermentans* gen. nov., sp. nov., a piezophilic, thermophilic, anaerobic, fermentative bacterium isolated from a deep-sea hydrothermal vent, Int. J. Syst. Evol. Microbiol., 65 (2014) 710–715.
[42] W.B. Hania, A. Postec, T. Aullo, A. Ranchou-Peyruse, G. Erauso, C. Brochier-Armanet, M. Hamdi, B. Ollivier, S. Saint-Laurent, M. Magot, M.L. Fardeau, *Mesotoga infera* sp. nov., a mesophilic member of the order *Thermotogales*, isolated from an underground gas storage aquifer, Int. J. Syst. Evol. Microbiol., 63 (2013) 3003–3008.
[43] K.A. Deweerd, L. Mandelco, R.S. Tanner, C.R. Woese, J.M. Suflita, *Desulfomonile tiedjei* gen. nov. and sp. nov., a novel anaerobic, dehalogenating, sulfate-reducing bacterium, Arch. Microbiol., 154 (1990) 23–30.
[44] Y.G. Zhao, Y. Zhang, Z. She, Y. Shi, M. Wang, M. Gao, L. Guo, Effect of substrate conversion on performance of microbial fuel cells and anodic microbial communities, Environ. Eng. Sci., 34 (2017) 666–674.
[45] S. Scheller, H. Yu, G.L. Chadwick, S.E. Mcglynn, V.J. Orphan, Artificial electron acceptors decouple archaeal methane oxidation from sulfate reduction, Science, 351 (2016) 703–707.
[46] J. Palatsi, J. Illa, F.X. Prenafeta-Boldú, M. Laureni, B. Fernandez, I. Angelidaki, X. Flotats, Long-chain fatty acids inhibition and adaptation process in anaerobic thermophilic digestion: batch tests, microbial community structure and mathematical modelling, Bioresour. Technol., 101 (2010) 2243–2251.

Supplementary information

Table S1
Trace element of nutrient solution

	Composition	Amount (g/L)	Composition	Amount (g/L)
Nutrient solution 1	EDTA	15.00	H_3BO_3	0.014
	$ZnSO_4{\cdot}7H_2O$	0.42	$CoSO_4{\cdot}7H_2O$	0.28
	$CuCl_2{\cdot}2H_2O$	0.17	$MnSO_4{\cdot}H_2O$	0.85
	$NiSO_4{\cdot}6H_2O$	0.21	$(NH_4)_2MoO_4$	0.20
Nutrient solution 2	EDTA	15.00	$FeSO_4{\cdot}7H_2O$	5.00

Table S2
Operation stages of the AFB–MFC system

Influent concentration mg/L	Phase 1					Phase 2		
	I	II	III	IV	V	VI	VII	VIII
COD	6,000	6,000	6,000	6,000	6,000	4,800	3,600	2,400
SO_4^{2-}	900	1,800	3,600	5,400	7,200	7,200	7,200	7,200
COD/SO_4^{2-}	6.7	3.3	1.7	1.1	0.83	0.67	0.50	0.33